Chapter 7

Adsorption of Metal Clusters on Graphene and Their Effect on the Electrical Conductivity

Roxana M. Del Castillo and Luis E. Sansores Cuevas

Additional information is available at the end of the chapter

http://dx.doi.org/10.5772/67476

Abstract

When adsorbates are introduced in graphene, the electric conductivity is highly modified. This chapter discusses how to estimate the electrical conductivity of graphene sheets with adsorbates, using electronic structure calculations and some theoretical approaches. Also, we discussed how the clustering of adsorbates attached to the graphene can impact electrical conductivity. We will focus in using metallic clusters as adsorbates (M_n; M = Ag, Au, Pt, and Pd; n = 1, 2, 3, and 4). The electrical conductivity is found using theoretical approaches, which are summarized in this chapter. We compare these approaches between each other to determine which is the most appropriate for each system.

Keywords: graphene, metallic clusters adsorption, conductivity

1. Introduction

It is well known that the experimental measurements of electrical conductivity are not so complicated; this is done with a four-point method to measure the sheet resistivity or conductivity [1, 2]. However, making a theoretical estimate of the electrical conductivity requires complicated mathematical elements, e.g., Lippmann-Schwinger equation [3, 4]. But there are some analytical methods based on Green's function to estimate the theoretical conductivity of pure graphene [5–8]. These methods can be extrapolated to estimate the conductivity of graphene with adsorbates or vacancies. The main advantage of these methods consists in that the conductivity can be calculated with structural parameters (deformation radius and heights). We propose to use these approximations to estimate the conductivity of graphene with the adsorption of metallic clusters (transition metal clusters).

By studying the way in which adsorption occurs, we can obtain strong elements to predict the behavior of the electrons into the graphene, wherein the scattering centers will be modeled as

potential steps in a two-dimensional waveguide. We consider that, when introducing the adsorbate in the graphene, the size of the scattering centers increases. If there is physisorption, the scattering centers are small, i.e., the potential step is small, and a good number of electrons can pass without scattering. If there is chemisorption, the scattering centers grow, so the potential step in the waveguide will increase in size and hinder the passage of electrons, causing more electrons to be scattered. This phenomenon of the creation of scattering centers is directly seen in the deformation of the graphene sheet, since the adsorption sites break the two-dimensionality of the graphene sheet, creating obstacles for the electrons and near the adsorption zone the sp_2 hybridization is broken, creating a clearly deformation of the graphene network.

The novelty of this work is to propose a direct methodology to estimate the electrical conductivity directly from calculations of electronic structure, in particular, optimized geometries. This methodology will allow a significant simplification of the theoretical calculations of conductivity. Recently, it has been reported that pure graphene has theoretical conductance and conductivity, but so far it has done anything on systems with dopants, and even more, on systems doped with metal clusters. Also, it consists of having direct applications in the field of nanoelectronic devices, catalytic materials, molecular electronics, developed sensors, and solar cells.

1.1. Review overview

Since the experimental production of graphene in 2004 by Novoselov et al. [9], graphene has been much studied by the scientific community. From the first moment, graphene presented an outstanding electronic behavior, since its electrons behave like Dirac Fermions with an effective speed around 10^6 m/s [10], reaching the regimes of electronic ballistic transport. Graphene has a minimum conductivity with a theoretical value of $e^2/\pi h$ (per valley per spin) [11], but the minimum conductivity measured experimentally is e^2/h (per valley per spin); this is known as the *missed-π-problem*. In 2007, Miao et al. [12] solved the problem by measuring the conductivity of small pieces of graphene as a function of an applied voltage, and to these pieces of graphene were changed the length and depth. They concluded that the theory is true, but only for small sheets. In addition to this, it is known that the mobility of graphene depends slightly on temperature and has a characteristic V-behavior [13]. The fact that electronic mobility depends slightly on temperature caused the theoretical conductivity of graphene to be investigated. In 2010, Barbier et al. [14] published a review where they calculated the theoretical conductivity of graphene in the limit of δ-function barriers. Recently, Kolasiński et al. calculated the conductivity with the Lippmann-Schwinger equation [15], and Garcia et al. published a theoretical approximation of graphene conductivity using the Kubo-Bastin approach [16]. In 2015, Kirczenow [17] calculated the scattering state wave functions of electrons on graphene nanostructures with the Lippmann-Schwinger equation, and he observed that when the Fermi energy is around the Dirac point (tunneling regimen), there is an inversion symmetry breaking to take into account. There is an alternative picture to describe the conductivity of graphene, Green function formalism with a different type of potential. In 2006, Ando [18] described graphene as a two-dimensional waveguide, where the impurities are treated as Coulomb

centers. The main advantage of treating impurities as centers of Coulomb is that it allows to propose in the equations a potential with long-range terms. However, this description was not enough, and there are other more sophisticated descriptions, e.g., graphene is developed as different regions of interest, connecting with self-energy terms in the Green function [19]; or three-terminal equilibrium Green's functions are used to determine the transmission phenomenon [20], using the structural parameters and boundary condition of graphene. In this chapter, will address three alternative approaches mention before, based on structural parameters and a Green function with a long-range potential. The three approximations present a behavior very similar to experiments being able to describe numerically the behavior at several temperatures.

However, for electronic devices, it is important to find the materials with good electrical conductivity and with an energy gap. When doping occurs to graphene, it is introduced as an energy gap and in some cases, continues to maintain a high electrical conductivity [21]. Mainly, the doping by the adsorption of atoms or clusters has been a well-supported way, since by means of the adsorbates the electronic and structural properties of the graphene can be modified. For example, introducing nitrogen atoms to the graphene surface induces a N-type doping, while by introducing oxygen atoms to the graphene, the Fermi energy remains at the point of Dirac (i.e. undoped) [22]. Depending on the adsorbate on the graphene, will be the type of interaction present in the system. Graphene with Cu, Ag atoms are adsorbed weakly on the surface of the graphene [23–25], whereas graphene with Pd are strongly adsorbed [25, 26]. It is of interest, to see that when doping the graphene with different adsorbate, we modify the electronic transport in the system, in particular, the conductivity [27]. In 2015, Liu et al. [28] distributed randomly weighted atoms on a sheet of graphene, this in order to modify the electronic transport, and they estimated the conductivity with the Kubo-Bastin formula. On the other hand, the studies made with graphene and adsorbates have been extrapolated to surface of high-quality boron and nitrogen co-doped graphene on silicon carbide substrate [29], indicating that these studies are important for the field of electronic devices.

2. Some theoretical conductivity approaches

In this chapter, we estimate conductivity with three approaches: frozen ripples approach (FRA), charged impurities scattering approach (CISA), and resonant scattering approach (RSA).

2.1. Frozen ripples approach (FRA)

In the frozen ripples approach (FRA), the main idea consists in using the deformation as a scattering center and then calculated the conductivity. Katsnelson and Geim [5] probed that in pure graphene, the scattering of the electrons behaves like as a controlled ripple introduced into the graphene surface (microscopic corrugations of a graphene sheet). They used the fact that certain types of ripples create a long-range scattering potential, as if they were Coulomb scatters, and provide charge-carriers almost independent of carrier concentration. Specifically, electrons are dispersed by a potential proportional to the square of the local curvature of

graphene. If electrons are scattered, then the resistivity increases, diminishing the ballistic behavior. Katsnelson and Geim approximated the excess of conductivity as follows:

$$\delta\sigma \approx \frac{4e^2}{h}\,\frac{a^2R^2}{z^4} \tag{1}$$

where z and R are the characteristic height and radius of ripples, respectively. In graphene with adsorbates, the scattering centers would be defined in the function of the adsorption properties (see Section 4).

2.2. Charged impurities scattering approach (CISA)

Once again, Katsnelson with Guinea and Geim analyzed how electrons in graphene, behaving like Dirac fermions, are scattered by clusters of charged impurity clusters [6]. Likewise, they showed that for graphene with a very low doping level, in some cases, the disorder increase the conductivity [6], and for the graphene with impurities, the disorder occurs in the form of large circular clusters, losing the scattering cross section, in comparison with isolated single atoms [7], and conductivity could be in ballistic regimen. The experimental manifestation of this phenomenon is observed as an increasing in the mobility [9–11, 13] at different temperatures. In these theories, there are two regimes:

- $k_F R << 1$ (the cluster is small compared to the Fermi wavelength), thus weakly perturbing the electronic wave function, and the adiabatic approximation can be used to obtain a constant value for $\sigma \propto k_F R^2 \left(\frac{V}{\hbar v_F R^{-1}}\right)^2$,
- $k_F R >> 1$ in this point is the cross section that is a function of the incident angle θ and the total cross section. The resonances are associated with the quasibound states inside the cluster. The conductivity (σ) is a function of Fermi wavelength (k_F), the potential (V), the Fermi velocity (v_F), the cluster concentration density (n_c), and the distortion radius (R) to the fourth power.

$$\sigma = \frac{e^2}{h} k_F l \sim \begin{cases} \dfrac{e^2}{h}\dfrac{1}{n_c R^2}\left(\dfrac{\hbar v_F R^{-1}}{V}\right)^2, & k_F R \ll 1 \\ \dfrac{e^2}{h}\left(\dfrac{k_F^2}{n_c}\right)^2, & k_F R \gg 1 \end{cases} \tag{2}$$

2.3. Resonant scattering approach (RSA)

Wehling et al. [8] used the semiclassical Boltzmann theory to calculate conductivity with a linear dependence of the carrier density. The principal scattering mechanism used is the midgap states [30] in the scattering mechanism. This mechanism is designed to describe the material defects as boundaries, cracks, adsorbates, or vacancies because these materials' defects induced a high potential difference with respect to the graphene sheet. Therefore, the phase shift tends to zero for wave vectors near to the Dirac point. If we considered a short-range contact potential, the behavior of the phase shift is logarithmic. In some instances, when the Fermi energy of the graphene-adsorbates is close to the Dirac point, it appears as a

http://dx.doi.org/10.5772/67476

resonance [31]. It is possible to compute the conductivity, using Boltzmann equation and the T matrix $\sigma \approx \left(\frac{2e^2}{h}\right)\left(2\pi n_i \left|\frac{T(E_F)}{D}\right|^2\right)^{-1}$, with $D = \sqrt{\sqrt{3}\pi}t$, and t is the nearest-neighbor hopping parameter. In the limit of resonant impurities, conductivity is,

$$\sigma \approx \left(\frac{4e^2}{\pi h}\right)\frac{n_e}{n_i}\, ln^2\left|\frac{E_F}{D}\right|, \tag{3}$$

$n_e = {}^{E_F^2}/_{D^2}$ is the number of charge carriers per carbon atom. The deformation radius is $D = hv_F/R$; the R parameter is seen directly to the geometry optimization; and $v_F = \sqrt{2E_F/m_e}$. For pure graphene, in a ballistic regimen, the Boltzmann approach becomes questionable because the quantum correction is predominant. However, small clusters has been proved to be sufficient to estimate conductivity of the graphene sheets with the adsorption of the metallic clusters [25].

3. Principal aspects of adsorption of metallic clusters on graphene

In this section, we examine the adsorption process of metallic clusters on graphene. We give some general trends, utilizing some specific systems to exemplify the adsorption phenomenon. The main features that will be studied in this section are ground-state properties, adsorption sites, adsorption energies, and density of states.

3.1. Ground states, adsorption sites, and adsorption energies

The first characteristic to study is the adsorption energy, which indicates if physisorption or chemisorption is occurring. In the next step, the adsorption site and how the deformation occurs in terms of the adsorption sites are observed. It is important to see under what conditions the deformation occurs, and the study of the adsorption sites gives us the radius and height of the scattering centers. The radius and heights are introduced into the three approaches to estimate the electrical conductivity. For physisorbed systems, the deformation is very low (small radius and height). For chemisorption systems, the deformation increases because the graphene feels strongly the metallic clusters.

To find the ground-state structures, adsorption sites, and adsorption energies, we optimized all our systems using a graphene sheet as a 6 × 6 supercell with a periodic condition in z-axis of 30 Å. All initial positions of the graphene systems with the clusters are listed below:

1. For one metal atom, the atom was placed in a top-site, right in the middle of the graphene sheet, over a distance of 3 Å (**Figure 1**).
2. For the dimer case, there are two possible positions: two metallic atoms at the same height forming a horizontal line and two metallic atoms aligned over a carbon atom forming a vertical line (**Figure 2**).

3. For the trimer case, there exists four possible positions: three metallic atoms at the same height conforming a horizontal line; three metallic atoms aligned over a carbon atom conforming a vertical line; three metallic atoms are at the same height, outlining a horizontal triangle over the graphene sheet; and three metallic atoms modeling a vertical triangle, and the two metallic atoms are at the same height of two adjacent carbon atoms (**Figure 3**).

4. For the tetramer case, there are eight initial configurations: four metallic atoms at the same height in a horizontal line; four metallic atoms aligned with one carbon atom of the graphene sheet forming a vertical line; four metallic atoms at the same height forming a rhombohedral shape or a diamond-shape in a horizontal plane; four metallic atoms aligned at one carbon atom of the graphene sheet forming a rhombohedral shape or a diamond-shape in a vertical plane; four metallic atoms at the same height forming a planar triangle plus 1 shape or a Y-shape in a horizontal plane; four metallic atoms aligned at one carbon atom of the graphene sheet forming a planar triangle plus 1 shape or a Y-shape in a vertical plane; four metallic atoms aligned at two carbon atoms of the graphene sheet forming a planar triangle plus 1 shape or a Y-shape in a vertical plane; and a tetrahedral isomer (the base of the tetrahedron is close to the graphene sheet) (**Figure 4**).

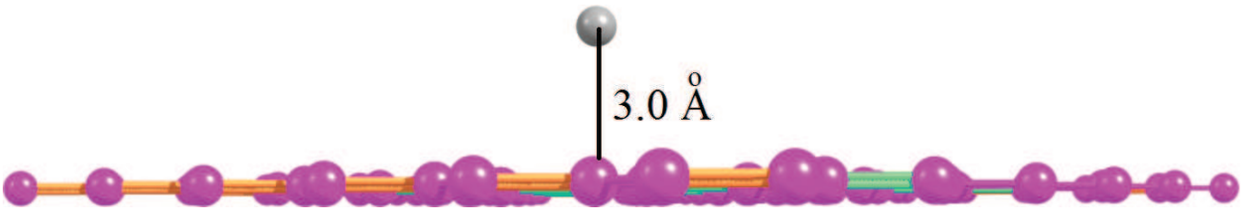

Figure 1. Initial position for one metal atom over a graphene sheet.

Figure 2. Initial position for a metallic dimer over a graphene sheet.

Figure 3. Initial position for a metallic trimer over a graphene sheet.

The computational calculations were performed with QUANTUM ESPRESSO computational package [32], and specifically performed DFT calculations using a plane wave basis set and pseudopotentials. The exchange and correlation interactions were carried out with the Perdew-Burke-Ernzerhof parameterization (GGA-PBE) [33]. The kinetic energy cutoff was taken as 40 Ry with a convergence criterion of 10^{-8} Ry. The Brillouin-zone integrations have been achieved with Methfessel–Paxton smearing special-point technique [34] centering de Γ point with a $4 \times 4 \times 1$

k-point mesh. The pseudopotentials of Ag and Pd were a Kr-like core; meanwhile, the pseudopotential of Au and Pt were Xe-like core. All the metals were approximate with smooth pseudopotentials generated with the Rappe-Rabe-Kaxiras-Joannopoulos (RRKJ) [35]. The adsorption energies have been computed with $E_a = E_{graphene + Mn} - (E_{graphene} + E_{Mn})$. The adsorption energies, the bond length from carbon to metallic atoms, and metallic atom to metallic atoms are presented in **Table 1** [25]. In this table, we indicate, in bold, the ground states. These ground states are taken to calculate the conductivity.

The ground-state system is shown in **Figure 5**. The systems with Ag and Au present that the Ag-Ag and Au-Au interactions are stronger than Ag-C and Au-C, the clusters almost do not

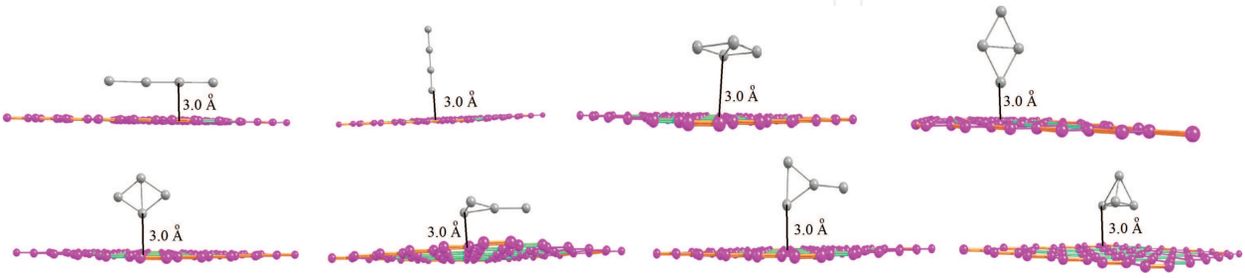

Figure 4. Initial position for a metallic tetramer over a graphene sheet.

		Graphene-Ag_n			**Graphene-Au_n**			**Graphene-Pt_n**			**Graphene-Pd_n**		
Structure	**n**	**d_{Ag-C}**	**d_{Ag-Ag}**	**E_a**	**d_{Au-C}**	**d_{Au-Au}**	**E_a**	**d_{Pt-C}**	**d_{Pr-Pt}**	**E_a**	**d_{Pd-C}**	**d_{Pd-Pd}**	**E_a**
Single atom	1	**3.26**		**−0.03**	**2.61**		**−0.31**	**2.09**		**−1.20**	**2.15**		**−1.20**
Horizontal line	2	Horizontal line convert in vertical line			Horizontal line convert in vertical line			3.87, 3.98	2.38	−0.14	2.13	2.70	−1.35
Vertical line	2	**2.63**	**2.58**	**−0.13**	**2.32**	**2.53**	**−0.64**	**2.23**	**2.41**	**−0.94**	**2.21**	**2.54**	**−0.65**
Horizontal line	3	Horizontal line convert in vertical line			Horizontal line convert in vertical line			3.94(2) 4.07	2.37(2)	−0.34	Horizontal line convert in horizontal triangle		
Vertical line	3	2.91	2.66(2)	−0.08	2.35	2.58, 2.56	−0.49	2.18	2.40, 2.42	−0.94	Vertical line convert in vertical triangle		
Horizontal triangle	3	3.34 3.33(2)	2.72(3)	−0.13	4.01 4.00(2)	2.69(3)	−0.34	3.89, 3.92, 3.97	2.51(3)	−0.54	3.90. 3.93. 4.08	2.51(3)	−1.80
Vertical triangle	3	**2.49 2.52**	**2.78, 2.70, 2.66**	**−0.36**	**2.34, 2.35**	**2.65 (2), 2.75**	**−0.75**	**2.17, 2.23, 4.55**	**2.53(2), 2.59**	**−1.82**	**2.13, 4.25, 4.32**	**2.46, 2.55(2)**	**−1.98**
Vertical line	4	2.63	2.62(2), 2.72	−0.053	2.36	2.54 (2), 2.60	−0.51	3.2	2.3(4)	−0.78	Vertical line convert in tetrahedral isomer		
Diamond shape horizontal	4	3.47, 3.67, 3.63, 3.62	2.75(2), 2.76(2), 2.64	−0.02	4.06, 4.07 (2), 4.11	2.66 2.69(4) 2.67	−0.17	3.98, 4.1(2), 3.98	2.53, 2.54(4)	−0.13	D-shape horizontal convert in tetrahedral isomer		

		Graphene-Ag_n			Graphene-Au_n			Graphene-Pt_n			Graphene-Pd_n		
Structure	**n**	$\mathbf{d_{Ag-C}}$	$\mathbf{d_{Ag-Ag}}$	$\mathbf{E_a}$	$\mathbf{d_{Au-C}}$	$\mathbf{d_{Au-Au}}$	$\mathbf{E_a}$	$\mathbf{d_{Pt-C}}$	$\mathbf{d_{Pr-Pt}}$	$\mathbf{E_a}$	$\mathbf{d_{Pd-C}}$	$\mathbf{d_{Pd-Pd}}$	$\mathbf{E_a}$
Diamond shape vertical	4	5.1(2), 2.74, 3.64	2.66, 2.72, 2.74(2), 2.76	−0.002	2.72, 5.00 (2), 7.34	2.67, 2.69 2.70(3)	−0.14	2.22, 4.27, 4.31, 6.17	2.52 (2),2.55 (2),2.58	−0.89	D-shape vertical convert in tetrahedral isomer		
Diamond Shape Vertical 1	4	2.56, 4.07, 4.2 5.2	2.70(2), 2,81(2), 2.65	−0.240	2.33, 4.00, 4.20, 4.97	2.63 2.65 (2), 2.78(2)	−0.44	2.49(2) 2.61(2) 2.53	2.23, 3.79(2) 4.7	−0.86	D-shape vertical convert in tetrahedral isomer		
Y-shape horizontal	4	3.59, 3.44, 3.75, 3.87	2.62, 2.63, 2.76, 2.62	−0.05	3.89, 3.92(3)	2.62, 2.69(2) 2.54	−2.47	4.08 (3), 4.13	2.37, 2.47, 2.52(2)	−0.25	Y-shape horizontal convert in tetrahedral isomer		
Y-shape vertical	4	3.33 (2), 5.83, 8.45	2.63(2), 2.75, 2.77	−0.05	Y-shape vertical convert in Y-shape vertical 1.			2.22 (2), 4.50, 6.90	2.52(2) 2.58, 2.41	−0.84	Y-shape vertical convert in tetrahedral isomer		
Y-shape vertical 1	4	**2.48, 4.27 (2), 5.03**	**2.61, 2.63, 2.76(2)**	**−0.30**	**2.32, 4.18, 4.57, 4.93**	**2.55, 2.61, 2.67, 2.70**	**−0.66**	2.25, 3.93, 4.10, 4.72	2.37, 2.47, 2.51, 2.58	−1.14	Y-shape vertical convert in tetrahedral isomer		
Tetrahedral	4	Tetrahedral isomer convert in D-shape horizontal			Tetrahedral isomer convert in D-shape horizontal			**2.17, 2.20, 3.80, 4.64**	**2.53, 2.65(2) 2.66(3)**	**−1.27**	**2.19, 3.83, 4.44, 4.77**	**2.55, 2.57(2) 2.62, 2.66(2)**	**−0.61**

All the distances are in Å, the adsorption energies (E_a) are in eV, and n is the number of atoms of the clusters. The ground states are presented in bold letter.

Table 1. Optimized geometries and adsorption energies of Ag, Au, Pt, and Pd clusters are supported on graphene.

distort the graphene surface. Meanwhile, the systems with Pd and Pt show that the interactions Pt-C and Pd-C is stronger than Pt-Pt and Pd-Pd, the clusters distorts very much the graphene sheet, and they settle into a valley created by them.

From the adsorption energies, adsorption sites, and the bond lengths, the most stable system is the trimer metallic cluster. The stability depends, mostly, in the covalent atomic radius. When the covalent atomic radius is smaller, the metallic atom can be accommodated between a carbon-carbon bond, distorting the graphene network. It is energetically favorable that the metallic atoms stick together and form clusters than to be separate between them onto the surface.

3.2. Electronic structure

The density of states (DOS) indicates how the adsorbates modified the type of doping in the systems. There are two charge transfer mechanisms observed in the density of states and in the population analysis [36], and these mechanisms are given in terms of the highest occupied orbital (HOMO) and the lowest unoccupied orbital (LUMO) of the adsorbates:

http://dx.doi.org/10.5772/67476

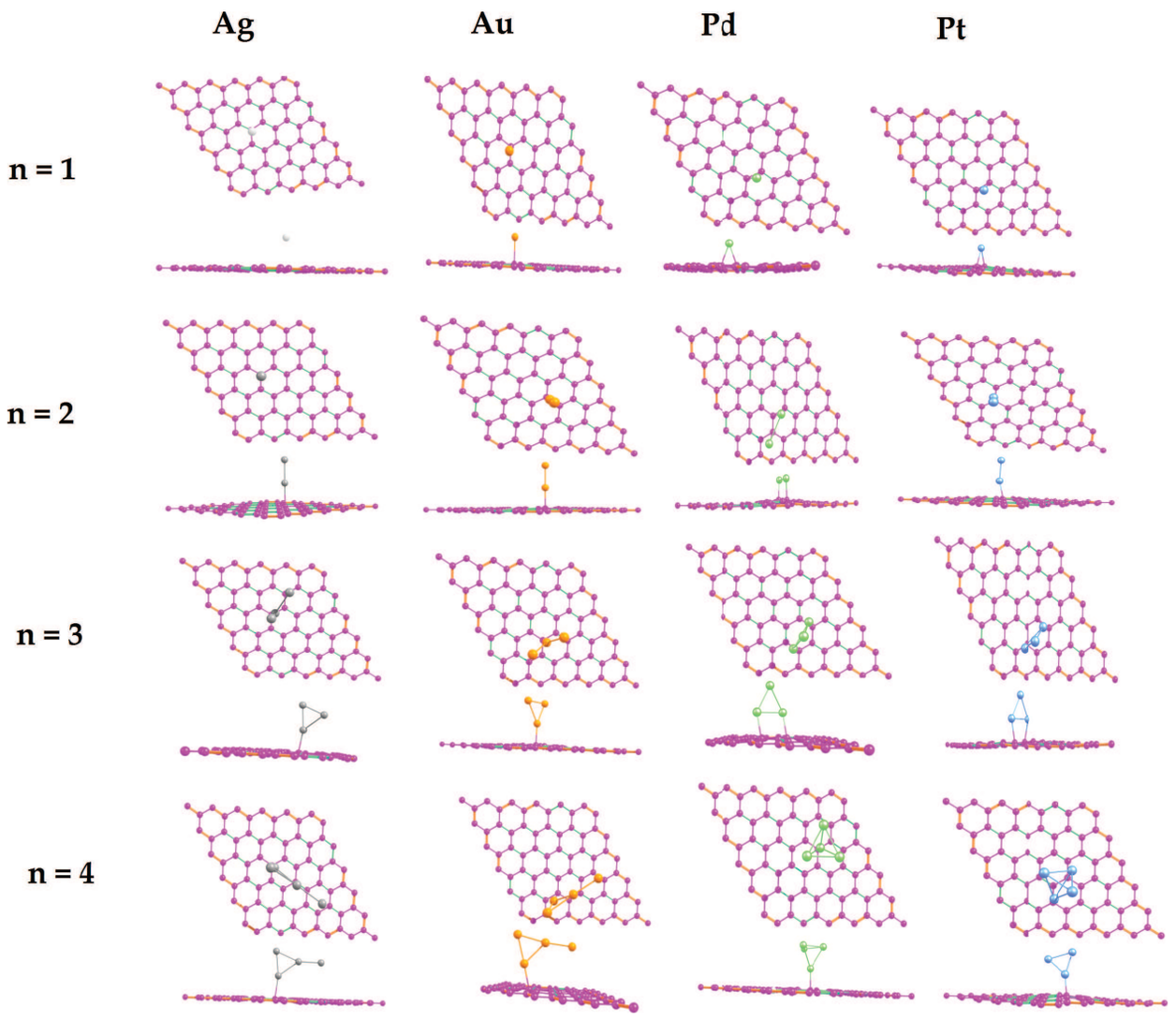

Figure 5. Ground-state structures of graphene-M_n (M = Ag, Au, Pt, and Pd; n = 1, 2, 3, and 4) [25].

- When the HOMO exceeds the Dirac point, the Fermi level of pure graphene occurs that the charge transfer goes from the cluster to the graphene. When the LUMO is below the Dirac point, the charge will transfer from the graphene to the cluster.
- When the charge transfer occurs between the cluster and the graphene sheet, this charge transfer is partially determined by the mixing of HOMO and LUMO orbitals (due to the hybridization).

The density of states (DOS) indicates how the charge transfer occurs and gives us a good supposition of how many free states are available to contribute to the conductivity. Also, indicates to us how the structure has been modified in terms of electronic behavior. For other side, the DOS is not conclusive to determine the conductivity, and we need other mechanism to complete the description.

The DOS of pure graphene has two basic properties: the DOS has a linear dependence of the energy around the Dirac point; and there are two Van Hove singularities around the Γ point, in

the Brillouin zone. When we introduced adsorbates, the Van Hove singularities displace away from the Γ point, and the DOS is modified and the Fermi level is shifted away from the Dirac point. The graphene-Ag_n (**Figure 6**) and graphene-Pt_n (**Figure 8**) are P-type doping, in which the charge is transferred from the graphene to the metallic clusters. Meanwhile, the graphene-Au_n (**Figure 7**) and graphene-Pd_n (**Figure 9**) are N-type doping, and the charge is transferred from the metallic cluster to the graphene surface.

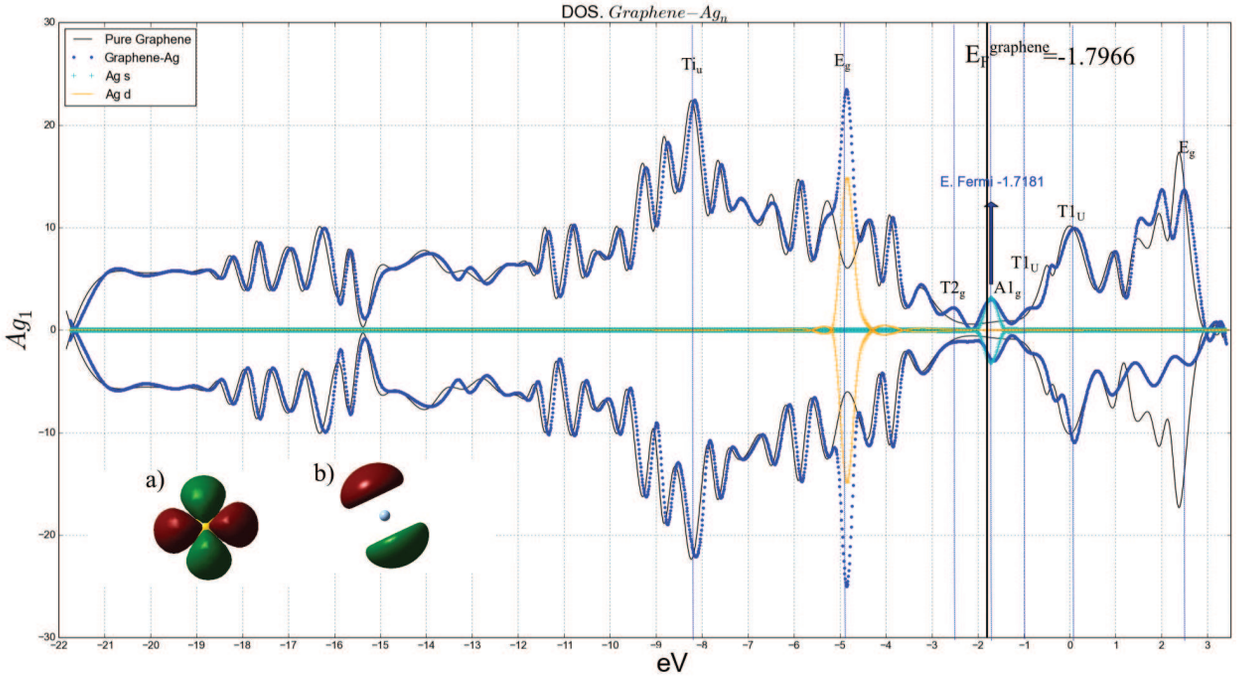

Figure 6. DOS of graphene-Ag_1 systems. Pure graphene is presented in a black line. The Dirac point is presented in −1.79 eV. It is presented the contributions of the MOs of Ag_1 are indicated with dotted lines [25], (a) the HOMO of Ag_1 and (b) the LUMO of Ag_1.

With the density of states, we can see the metallic cluster orbitals that distort the density of states of pure graphene. By distorting the density of states, the electronic transport properties are modified. For graphene-Ag_n systems, the silver cluster has that its 5s states are very close to the Fermi energy, contributing directly to the electronic transport. In the particular case of a single silver atom on the surface of graphene (Graphene-Ag), the 6s state of the silver enters directly into the Fermi energy, which causes states to fill up and improves electronic transport. For graphene-Pt_n systems, the 6s states of platinum enter the border orbitals, mostly in the LUMO, whereas the 5d orbitals enter the HOMO orbital. Both graphene-Ag_n and graphene-Pt_n present P-type doping and their orbital p is not present in the transport of charge. For systems with N-type doping, it is seen that the orbitals involved in the transfer of charge remain the orbital s and d of metallic clusters. Although in these cases, the contribution of the p orbitals of the metallic clusters in the virtual orbitals of the final structure is already perceived. To see more detail, we recommend the article [25]

http://dx.doi.org/10.5772/67476

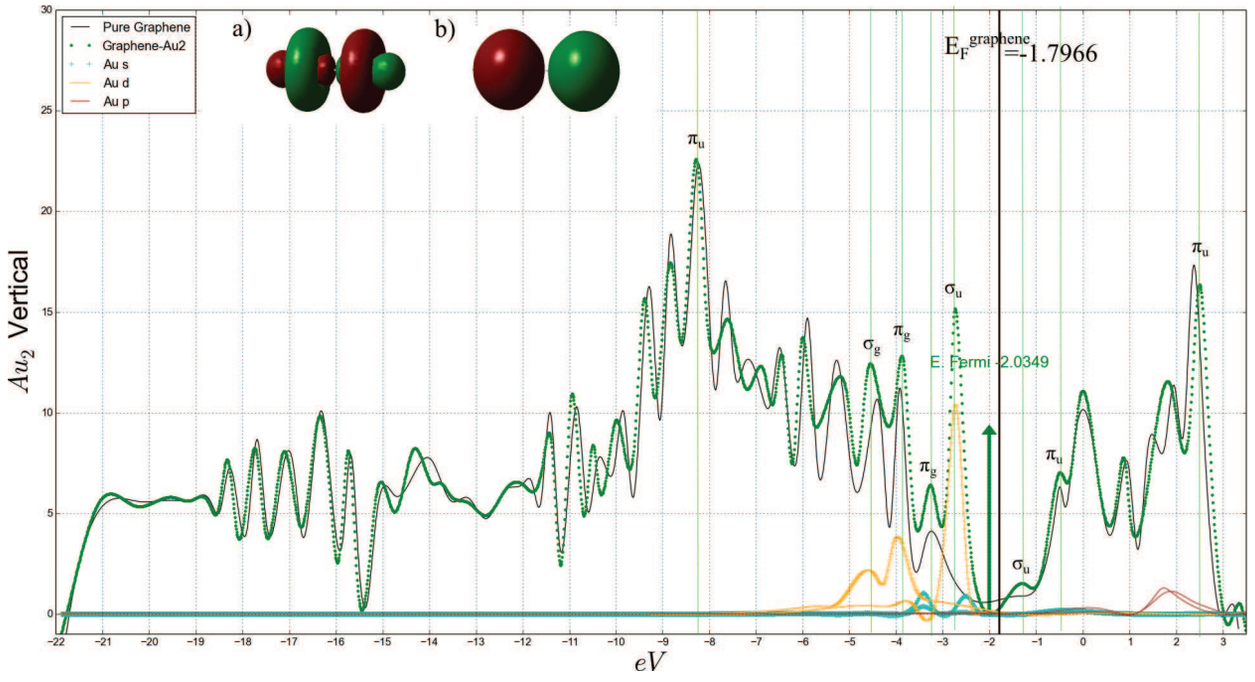

Figure 7. DOS of graphene-Au2 systems. Pure graphene is presented in a black line. The Dirac point is presented in −1.79 eV. It is presented the contributions of the MOs of Au_2 are indicated with dotted lines [25], (a) the HOMO of Au_2 and (b) the LUMO of Au_2.

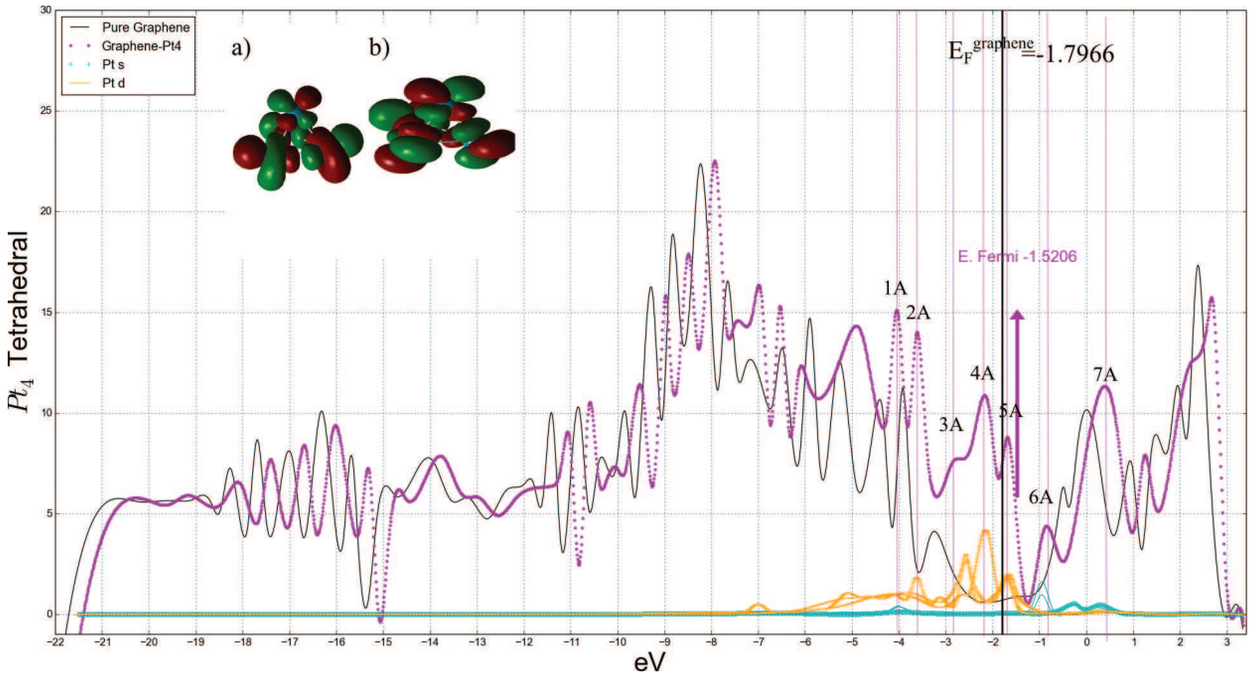

Figure 8. DOS of graphene-Pt_4 systems. Pure graphene is presented in a black line. The Dirac point is presented in −1.79 eV. It is presented the contributions of the MOs of Pt_4 are indicated with dotted lines [25], (a) the HOMO of Pt_4 and (b) the LUMO of Pt_4.

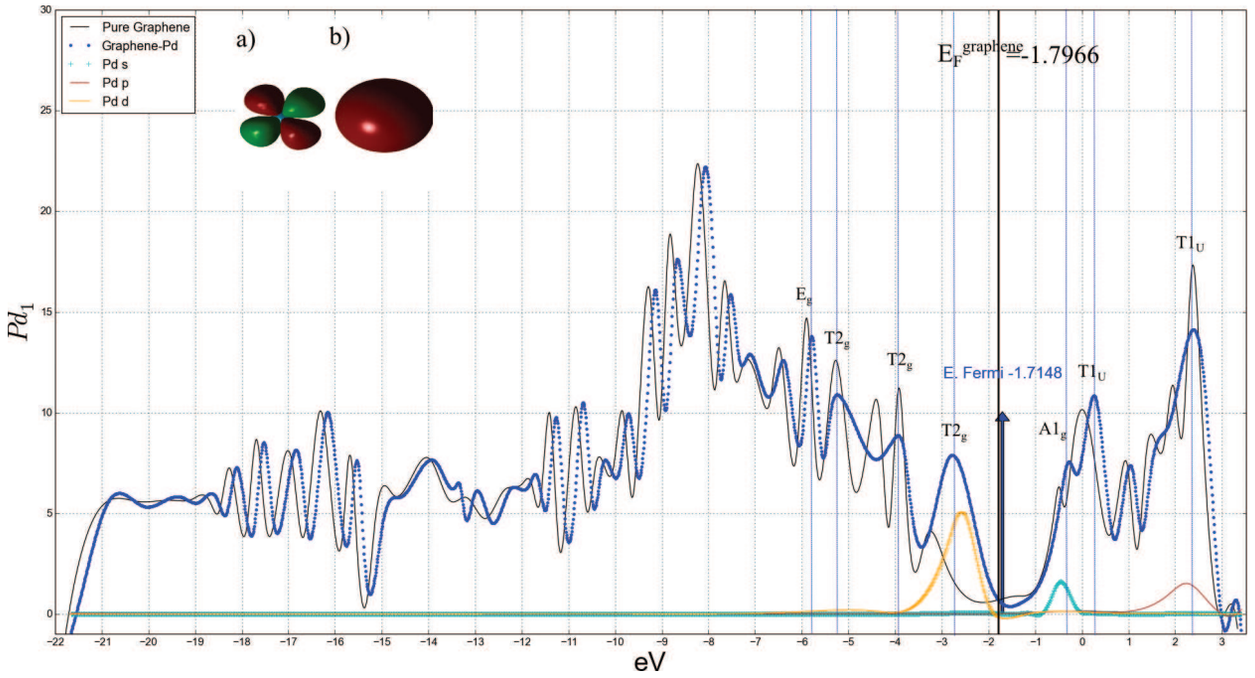

Figure 9. DOS of graphene-Pd_1 systems. Pure graphene is presented in a black line. The Dirac point is presented in −1.79 eV. It is presented the contributions of the MOs of Pd_1 are indicated with dotted lines [25], (a) the HOMO of Pd_1 and (b) the LUMO of Pd_1.

4. Conductivity

We used the approaches from Section 2 to estimate the conductivity of the graphene with metallic adsorbates. To calculate the conductivity or conductance of the graphene with adsorbates, it is necessary to follow the next steps:

1. Optimized the geometry. When we optimized the geometry, in most computational package, we obtained the Fermi Energy E_F and the deformation. With the Fermi energy, it is possible to estimate v_F ($v_F = \sqrt{2E_F/m_e}$, m_e is the electron mass). The deformation is directly obtained with the coordinates of the final structure. Specifically, the deformation is obtained with the adsorption radius and height of the sheet of graphene produced by the adsorption, i.e., the graphene surface is placed in the $z = 0$ plane, the metallic cluster will pull to the surface, this distance is to what we call height. The deformation radius takes us to the distance between the minimum height and the maximum height around the adsorbate. Other method to obtain the deformation is with the charge density surface (CDS); the CDS displays the scattering section due to the adsorption of the metal cluster on the graphene sheet. With the CDS, it is possible to obtain the deformation radius (see **Figure 10**) [37].

2. Determine which approach will be used:

   a. Evaluate the gap between the Dirac point and the Fermi Energy of the graphene-M_n systems $|\varepsilon - E_F|$ (see **Table 2**). If E_F of the adsorbed system is closed to Dirac point $|\varepsilon - E_F| = 0$, the more convenient approach to used is RSA.

http://dx.doi.org/10.5772/67476

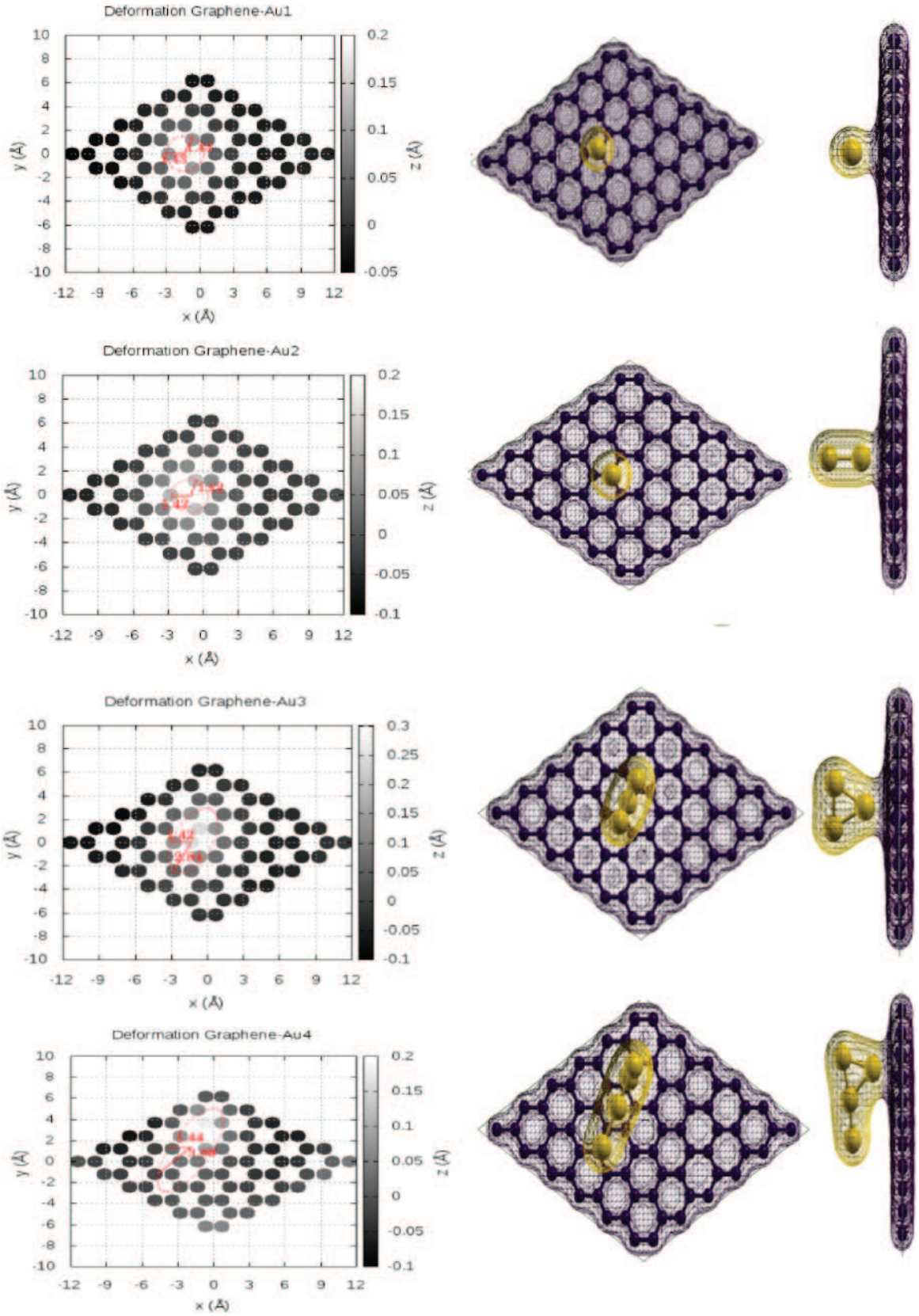

Figure 10. Optimized geometry of graphene-Au_n. It shows the deformation produced by the adsorption of the golden cluster with the coordinates and with the charge density surface (CDS) [25, 37].

b. If we are going to use CISA, it is important to determine which is the regimen that we are going to use. This is done by calculating the $k_F R$ parameter. For our systems, we have $k_F R \approx (1.6 - 3.05) \times 10^{-19} \ll 1$ for 1.4Å ≤ R ≤ 2.7Å.

3. Obtain the adsorption energy, which can be used as of the V potential in CISA (suppose the graphene sheet as a two-dimensional wave guide with a step potential as the scattering center).

4. For RSA, it is imperative to determine the cluster concentration n_c. We calculate n_c with the unit's supercell parameters (see **Figure 10**), for our systems, we have $n_c = 2.9 \times 10^{13}$ cm^2 for cluster. Likewise, it is necessary to calculate the parameter D, which is calculated in terms of v_F and the deformation radius (R), as $D = hv_F/R$,

Following these steps, it is possible to estimate the conductivity with one of the three available approaches (FRA, CISA, or RSA), see **Table 3**. It is important to notice, that in some cases, the deformation would be created in an ellipse center and not a circle center. In this case, the radius of deformation was taken as the average of the major and minor radii. The ellipse center is previously considered in bilayer graphene [38, 39].

$\lvert\varepsilon - E_F\rvert$ **(eV)**	**1**	**2**	**3**	**4**
Ag	0.0785	0.0987	0.7409	0.5436
Au	0.2434	0.2383	0.2830	0.0060
Pt	0.0413	0.2355	0.0171	0.2760
Pd	0.0798	0.0191	0.0457	0.2811

Table 2. Gap between the Dirac point (ε) and the Fermi Energy of the graphene-M_n systems $\lvert\varepsilon - E_F\rvert$.

			FRA		**CISA**		**RSA**			
System	**E_F [eV]**	**R [Å]**	**z [Å]**	**g [S/cm]**	**v_F [m/s]**	**V [eV]**	**g [S/cm]**	**D(R) [eV]**	**n_e/C-atom**	**g [S/cm]**
Graphene-Ag	−1.72	1.43	0.025	**148.78**	7.77×10^5	0.03	**128.53**	1.89	0.82	**153.27**
Graphene-Ag_2	−1.70	2.46	0.03	**23.34**	7.73×10^5	0.13	**60.73**	2.06	0.67	**47.94**
Graphene-Ag_3	−1.06	2.66	0.163	**6.03**	6.09×10^5	0.36	**3.60**	1.51	0.49	**14.18**
Graphene-Ag_4	−1.25	3.36	0.073	**1.24**	6.64×10^5	0.3	**2.49**	1.30	0.93	**21.32**
Graphene-Au	−2.04	1.43	0.020	**34.11**	8.47×10^5	0.31	**40.77**	3.90	0.27	**33.24**
Graphene-Au_2	−2.04	1.42	0.12	**12.16**	8.46×10^5	0.64	**27.05**	3.92	0.27	**15.63**
Graphene-Au_3	−1.51	2.13	0.25	**0.36**	7.30×10^5	0.75	**2.89**	2.25	0.45	**8.83**
Graphene-Au_4	−1.80	2.65	0.061	**1.63**	7.96×10^5	0.66	**1.86**	1.98	0.83	**13.00**
Graphene-Pt	−1.84	1.94	0.33	**0.15**	8.04×10^5	1.2	**1.99**	2.73	0.45	**6.09**
Graphene-Pt_2	−2.03	1.98	0.12	**6.78**	8.45×10^5	0.94	**3.32**	2.81	0.52	**9.67**
Graphene-Pt_3	−1.78	2.39	0.21	**1.27**	7.91×10^5	1.82	**0.37**	2.18	0.67	**3.23**
Graphene-Pt_4	−1.52	2.65	0.33	**0.19**	7.31×10^5	1.27	**0.42**	1.82	0.70	**4.32**
Graphene-Pd	−1.72	1.94	0.25	**1.04**	7.77×10^5	1.2	**1.86**	2.64	0.42	**5.54**
Graphene-Pd_2	−1.53	2.52	0.12	**9.93**	7.35×10^5	1.35	**4.62**	1.92	0.64	**4.01**

http://dx.doi.org/10.5772/67476

			FRA		CISA		RSA			
System	**E_F [eV]**	**R [Å]**	**z [Å]**	**g [S/cm]**	**v_F [m/s]**	**V [eV]**	**g [S/cm]**	**D(R) [eV]**	**n_e/C-atom**	**g [S/cm]**
Graphene-Pd_3	−1.76	2.27	0.21	**1.27**	7.85×10^5	1.98	**3.75**	2.28	0.59	**2.79**
Graphene-Pd_4	−1.52	2.66	0.145	**3.21**	7.30×10^5	0.61	**1.88**	1.81	0.70	**1.55**

The conductivity is present in bold letter [25].

Table 3. Parameters used to obtain the conductivity in the three approximations (FRA, CISA, and RSA).

We compare our results with some other experiments previously reported. For graphene-Ag system, the experimental conductivity value is of 155 Scm^{-1} [40], whereas our theoretical value is 148.78 Scm^{-1} with FRA, 123.53 Scm^{-1} with CISA, and 153.27 Scm^{-1} with RSA. The best approach for this system is RSA, consistently with a gap between the Dirac point and the

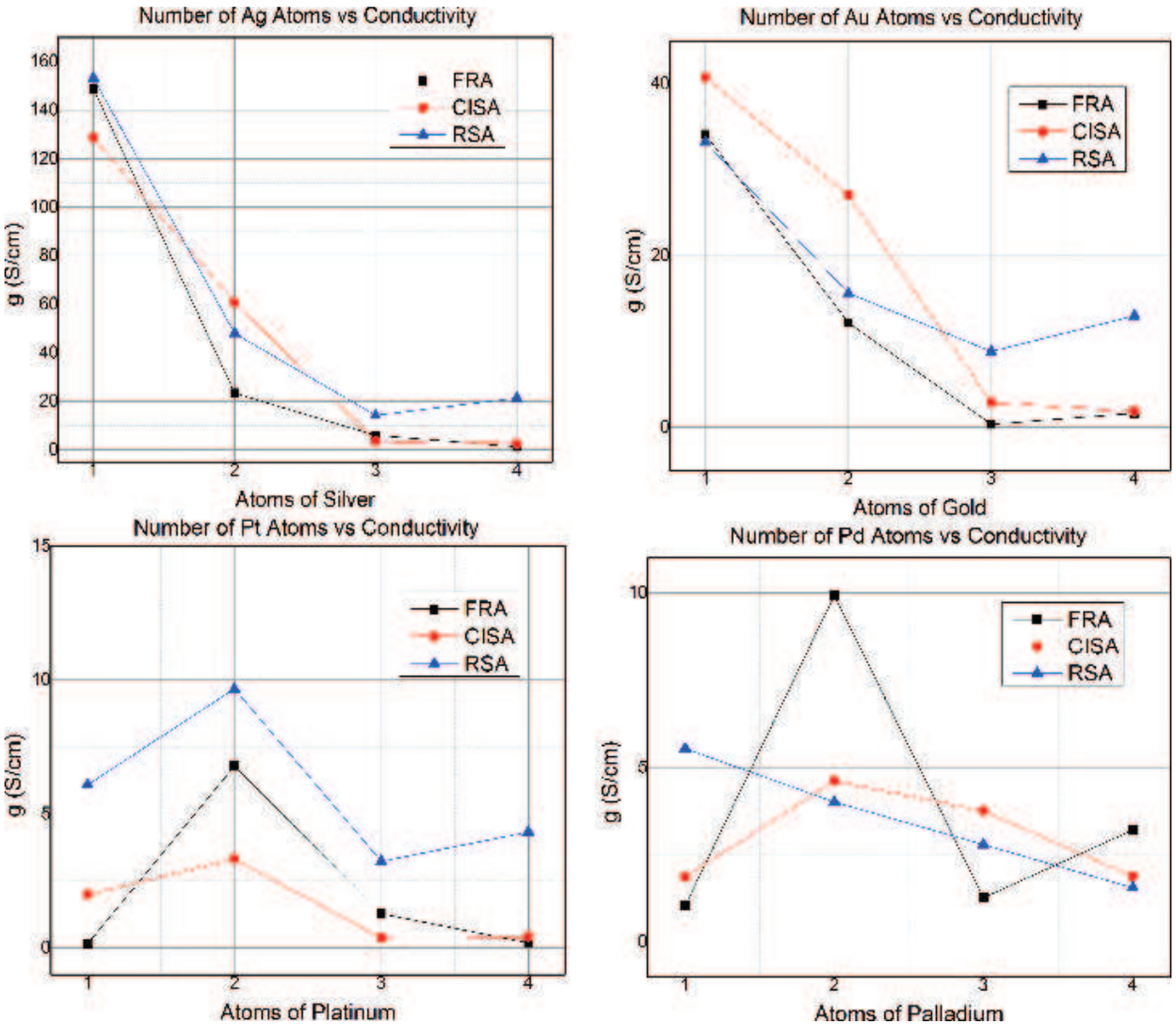

Figure 11. Conductivity of the graphene-Mn (M = Ag, Au, Pt, and Pd; n = 1, 2, 3, and 4) as a function of the number atoms. The conductivity is calculated with the FRA, CISA, and RSA approach [25]© The European Physical Journal.

Fermi Energy of 0.078 eV. In **Figure 11**, it is possible to observe the conductivity value for each system. We present the conductivity in the function of a number of atoms. It is evident that the conductivity decreases as the number increases for graphene-Ag_n and graphene-Au_n systems. Till the graphene-Pt_n systems have an even-odd behavior, i.e., for an even number of metallic atoms in the cluster, the conductivity increases. For the graphene-Pd_n systems, the behavior of the conductivity depends on the approach. It is important to notice that the graphene-Pd_1 system, graphene-Pd_2, and graphene-Pd_3 meet the condition of $|\varepsilon - E_F| = 0$, making the RSA approach more convenient than the others. Also for graphene-Pd_n, the RSA approach is the only approach with a linear curve giving us a little more confidence since it coincides with the behavior of the other metals.

In general terms, the FRA approximation is not exact but allows to estimate the conductivity in orders of magnitude, only with the ground-state geometry. The CISA is a good approach; it is designed for graphene with charged impurities, which would be our case. The main advantage is that it uses few parameters obtained from an optimization of the geometry. But nevertheless, do not consider midgap states. The RSA approach needs some little extra calculations, in addition to geometry optimization, but it seems to be the one that most closely approximates the experimental results.

5. Future trends and conclusions

It has been proposed that a simple method to make a qualitative estimation of the conductivity of graphene surfaces with dopants, leaving the conductivity as a function of the structural deformation of the graphene surface. The proposed method is based on three theoretical approaches (FRA, CISA, and RSA). The main advantage of this method is that the calculation of the conductivity is made from the optimized geometry and three approaches are used to calculate it.

From our calculations of conductivity, it is observed that the phenomenon of adsorption affects much the conductivity. The weak adsorption slightly affects the conductivity, whereas the strong adsorption causes the conductivity to decrease drastically. For weak adsorption, involving pure van der Waals forces, the FRA, CISA, and RSA approximations are quite acceptable since they predict conductivity in the same order of magnitude. However, for the strong adsorption, the situation changes, since these approximations are designed for graphene and when the chemisorption breaks the two-dimensionality of the graphene. The approximations are based on the fact that graphene is a two-dimensional waveguide, where the scattering centers are potential steps. These potential steps are of small value so that most of the electrons pass without being dispersed, and the ballistic conductivity is preserved. As the adsorbate enter the system, the size of dispersing centers increases. This phenomenon is presented in the method when we take the energy of adsorption as the value of potential step. It is recommended to be careful when applying approaches because if the Fermi energy is very close to the Dirac point, the only valid approach is RSA.

With respect to the adsorption of metallic clusters on graphene surfaces, it was observed that there are metallic clusters adsorbed in graphene that induces a band gap in the Fermi energies and conserved the high conductivity (graphene-Ag).

It is observed that the physisorbed systems on the surface of graphene have a lower deformation of the network and they have a high conductivity, as is the case of graphene-Ag_n, whereas the chemisorbed systems have a high deformation of the network and drastically reduced the conductivity, such as the graphene-Pt_n system. It was observed that it is important to consider the midgap states, since if they occur in our systems, we cannot use the simplest approximations to estimate the conductivity and we need to use RSA, which is the approximation that does consider these states (observe the case of graphene-Pd_n). It is also observed that there is no correlation between the type of doping and the conductivity of the material. The partial state density of the systems gives us the orbital of the metallic cluster that interact with the graphene and that directly modify the energy gap, necessary for the creation of transistors.

For future research, we propose conducting the conductivity measurement with more direct methods, such as conductivity measurement with Landauer-Büttiker. And compare it with our calculations presented here. It will also serve to understand, as fully as possible, the behavior of electronic transport. This can be done by looking at the energy bands and the transport coefficient, calculated with Landauer-Büttiker. It is also proposed that these results would be compared with experimental conductivity measurements. To carry out this, it is essential to know the process of production of the graphene samples, to understand what the type of doping would be and then to model the graphene sheet computationally to estimate the conductivity.

In an article made by Wehling et al., it was proposed to expand the RSA approximation into defective Graphene/h-BN hetero-structures [41]. Since in these structures, it is observed that there are states of midgap and band gap modification. We believe that these studies can be extrapolated to any two-dimensional surface in which impurities are joined by Van der Waals forces. This assumption will have to be verified posteriori.

Author details

Roxana M. Del Castillo* and Luis E. Sansores Cuevas

*Address all correspondence to: roxanadelcastillo@ciencias.unam.mx

Materials Research Institute, National Autonomous University of Mexico, Circuito Exterior, Campus Universitario, Mexico City, Mexico

References

[1] Lotz M.R., Boll M., Østerberg F.W., Hansen O., Petersen D.H. Mesoscopic current transport in two-dimensional materials with grain boundaries: Four-point probe resistance and Hall effect. Journal of Applied Physics. 2016;**120**(12), 134303:10.1063. DOI: http://dx.doi.org/10.1063/1.4963719

[2] Wang L., Meric I., Huang P.Y., Gao Q., Gao Y., Tran H., Taniguchi T., Watanabe K., Campos L. M., Muller D.A., Guo J., Kim P., Hone J., Shepard K.L., Dean C.R. One-dimensional electrical

contact to a two-dimensional material. Science. 2013;**342**(6158):614–617. DOI: 10.1126/science.1244358

[3] François Fillion-Gourdeau F., MacLean S. Time-dependent pair creation and the Schwinger mechanism in graphene. Physical Review B. 2015;**92**:035401. DOI: https://doi.org/10.1103/PhysRevB.92.035401

[4] Schneider M., Faria D., Viola Kusminskiy S., Sandler N. Local sublattice symmetry breaking for graphene with a centrosymmetric deformation. Physical Review B. 2015;**91**:161407 (R). DOI: https://doi.org/10.1103/PhysRevB.91.161407

[5] Katsnelson M.I., Geim A.K. Electron scattering on microscopic corrugations in graphene. Philosophical Transactions of the Royal Society A. 2008;**366**(1863). DOI: 10.1098/rsta.2007.2157

[6] Katsnelson M.I., Guinea F., and Geim A.K. Scattering of electrons in graphene by clusters of impurities. Physical Review B. 2009;**79**:195426. DOI: https://doi.org/10.1103/PhysRevB.79.195426

[7] Guinea F. Models of electron transport in single layer graphene. Journal of Low Temperature Physics. 2008;**153**(5):359–373. DOI: 10.1007/s10909-008-9835-1

[8] Wehling T., Yuan S., Lichtenstein A.I., Geim A.K., Katsnelson M.I. Resonant scattering by realistic impurities in graphene. Physical Review Letters. 2010;**105**(5):056802. DOI: https://doi.org/10.1103/PhysRevLett.105.056802

[9] Novoselov K.S., Geim A.K., Morozov S.V., Jiang D., Zhang Y., Dubonos S.V., Grigorieva I. V., Firsov A.A. Electric field effect in atomically thin carbon films. Science. 2004;**306** (5696):609–666. DOI: 10.1126/science.1102896

[10] Partoens B. and Peeters F.M. From graphene to graphite: Electronic structure around the K point. Physical Review B. 2006;**74**:075404. DOI: https://doi.org/10.1103/PhysRevB.74.075404

[11] Katsnelson M.I., Novoselov K.S. Graphene: New bridge between condensed matter physics and quantum electrodynamics. Solid State Communications. 2007;**143**(1–2):3–13. DOI: http://dx.doi.org/10.1016/j.ssc.2007.02.043

[12] Miao F., Wijeratne S., Zhang Y., Coskun U.C., Bao W., Lau C.N. Phase-coherent transport in graphene quantum billiards. Science. 2007;**317**(1530):1530–1535. DOI: DOI: 10.1126/science.1144359

[13] Morozov S.V., Novoselov K.S., Katsnelson M.I., Schedin F., Elias D.C., Jaszczak J.A., and Gei A.K. Giant intrinsic carrier mobilities in graphene and its bilayer. Physical Review Letters. 2008;**100**:016602. DOI: https://doi.org/10.1103/PhysRevLett.100.016602

[14] Barbier M., Vasilopoulos P., Peeters F.M. Single-layer and bilayer graphene superlattices. Philosophical Transactions of the Royal Society A. 2010;**368**:5499–5524. DOI: doi:10.1098/rsta.2010.0218

[15] Kolasiński K., Mreńca-Kolasińska A., and Szafran B. Theory of ballistic quantum transport in the presence of localized defects. Physical Review B. 2016;**94**:115406. DOI: https://doi.org/10.1103/PhysRevB.94.115406

[16] Garcia J.H, Rappoport T.G. Kubo–Bastin approach for the spin Hall conductivity of decorated graphene. 2D Materials. 2016;**3**(2). DOI: http://dx.doi.org/10.1088/2053-1583/3/2/024007

[17] Kirczenow G. Valley currents and nonlocal resistances of graphene nanostructures with broken inversion symmetry from the perspective of scattering theory. Physical Review B. 2015;**95**:125425. DOI: https://doi.org/10.1103/PhysRevB.92.125425

[18] Ando T. Screening effect and impurity scattering in monolayer graphene. Journal of Physical Society of Japan. 2006;**75**:074716. DOI: http://dx.doi.org/10.1143/JPSJ.75.074716

[19] Settnes M., Power S.R., Lin J., Petersen D.H., Jauho A. Patched Green's function techniques for two-dimensional systems: Electronic behavior of bubbles and perforations in graphene. Physical Review B. 2015;**91**:125408. DOI: https://doi.org/10.1103/PhysRevB.91.125408

[20] Jacobsena K.W., Falkenberga J.T., Papiora N., Bøggilda P., Jauhoa A.P., Mads Brandbyge M. All-graphene edge contacts: Electrical resistance of graphene T-junctions. Carbon. 2016;**101**:101–106. DOI: http://dx.doi.org/10.1016/j.carbon.2016.01.084

[21] McCreary K.M., Pi K., Swartz A.G., Han W., Bao W., Lau C.N., Guinea F., Katsnelson M. I., Kawakami R.K. Effect of cluster formation on graphene mobility. Physical Review B. 2010;**81**:115453. DOI: https://doi.org/10.1103/PhysRevB.81.115453

[22] Marsden A.J., Brommer P., Mudd J.J., Dyson M.A., Cook R., Asensio M. Effect of oxygen and nitrogen functionalization on the physical and electronic structure of graphene. Nano Research. 2015;**8**(8):2620–2635. DOI: 10.1007/s12274-015-0768-0

[23] Vanin M., Mortensen J.J., Kelkkanen A.K., Garcia-Lastra J.M., Thygesen K.S., and Jacobsen K.W. Graphene on metals: A van der Waals density functional study. Physical Review B. 2010;**81**:081408(R). DOI: https://doi.org/10.1103/PhysRevB.81.081408

[24] Amft M., Lebègue S., Eriksson O. and Skorodumova N.V. Adsorption of Cu, Ag, and Au atoms on graphene including van der Waals interactions. Journal of Physics: Condensed Matter. 2011;**23**(39). DOI: http://dx.doi.org/10.1088/0953-8984/23/39/395001

[25] Del Castillo R.M., Sansores L.E. Study of the electronic structure of Ag, Au, Pt and Pd clusters adsorption on graphene and their effect on conductivity. European Physical Journal B. 2015;**88**(248). DOI: http://dx.doi.org/10.1140/epjb/e2015-60001-2

[26] Lopez M.J., Cabria I., Alonso J.A. Palladium clusters anchored on graphene vacancies and their effect on the reversible adsorption of hydrogen. Journal of Physical Chemistry C 2014;**118**(10):5081–5090. DOI: 10.1021/jp410262t

[27] Hofmann M., Hsieh Y.P., Chang K.W., Tsai H.G, Chen T.T. Dopant morphology as the factor limiting graphene conductivity. Scientific Reports. 2015;**5**:17393. DOI: 10.1038/srep17393

[28] Liu Z., Zhu M., and Zheng Y. Quantum transport properties of graphene in the presence of randomly distributed. Physical Review B 2015;**92**:245438. DOI: 10.1103/PhysRevB.92.245438

[29] Telychko M., Mutombo P., Merino P., Hapala P., Ondráček M., Bocquet F.C, et al. Electronic and chemical properties of donor, acceptor centers in graphene. ACS Nano. 2015;**9** (9):9180–9187. DOI: 10.1021/acsnano.5b03690

[30] Stauber T., Peres N.M.R., and Guinea F. Electronic transport in graphene: A semiclassical approach including midgap states. Physical Review B. 2007;**76**:205423. DOI: https://doi.org/10.1103/PhysRevB.76.205423

[31] Guinea F., Katsnelson M.I. Many-body renormalization of the minimal conductivity in graphene. Physical Review Letters. 2014;**112**:116604. DOI: https://doi.org/10.1103/PhysRevLett.112.116604

[32] Giannozzi P., Baroni S., Bonini N., Calandra M., Car R., Cavazzoni C., et al. QUANTUM ESPRESSO: A modular and open-source software project for quantum simulations of materials. Journal of Physics: Condensed Matter. 2009;**21**(39). DOI: http://dx.doi.org/10.1088/0953-8984/21/39/395502

[33] Perdew J.P, Burke K., and Ernzerhof M. Generalized gradient approximation made simple. Physical Review Letters. 1996;**77**:3865. DOI: https://doi.org/10.1103/PhysRevLett.77.3865

[34] Methfessel M. and Paxton A.T. High-precision sampling for Brillouin-zone integration in metals. Physical Review B. 1989;**40**(3616)DOI: https://doi.org/10.1103/PhysRevB.40.3616

[35] Rappe A.M., Rabe K.M., Kaxiras E., and Joannopoulos J.D. Optimized pseudopotentials. Physical Review B. 1991;**41**:1227. DOI: https://doi.org/10.1103/PhysRevB.41.1227

[36] Masir, M.R., Leenaerts, O., Partoens, B., and Peeters, F.M. Theory of the Structural, Electronic and Transport Properties of Graphene. In: Houssa M., Dimoulas A., Molle A., editors. 2D Materials for Nanoelectronics. Boca Raton, FL, CRC Press; 2016. pp. 3–36. DOI: 10.1201/b19623

[37] Del Castillo R.M. Ballistic Conductivity in Graphene [thesis]. Mexico: UNAM; 2016. 134 p. Available from: http://132.248.9.195/ptd2016/enero/099083380/Index.html

[38] Katsnelson M.I., Scattering of charge carriers by point defects in bilayer graphene. Physical Review B. 2007;**76**:073411. DOI: https://doi.org/10.1103/PhysRevB.76.073411

[39] Lotfi E., Rezania H., Arghavaninia B., Yarmohammadi M. Impurity effects on electrical conductivity of doped bilayer graphene. Chinese Physics B. 2016;**25**(7):076102. DOI: 10.1088/1674-1056/25/7/076102

[40] Pasricha R., Gupta S., and Srivastava A.S. A facile and novel synthesis of Ag–graphene-based. Small. 2009;**5**(20):2253–2259. DOI: 10.1002/smll.200900726

[41] Sachs B., Wehling T.O., Katsnelson M.I., and Lichtenstein A.I. Midgap states and band gap modification in defective graphene/h-BN heterostructures. Physical Review B. 2016;**94**:224105. DOI: https://doi.org/10.1103/PhysRevB.94.224105